In search of quark gluon plasma in nuclear collisions

Jan-e Alam
Theoretical Physics Division, Variable Energy Cyclotron Centre, 1/AF, Bidhan Nagar, Kolkata - 700064, India

Abstract

At high temperatures and densities the nuclear matter undergoes a phase transition to a new state of matter called quark gluon plasma (QGP). This new state of matter which existed in the universe after a few microsecond of the big bang can be created in the laboratory by colliding two nuclei at relativistic energies. In this presentation we will discuss how the the properties of QGP can be extracted by analyzing the spectra of photons, dileptons and heavy flavours produced in nuclear collisions at Relativistic Heavy Ion Collider (RHIC) and Large Hadron Collider (LHC) energies.

1. Introduction

The theory of strong interaction - Quantum Chromodynamics (QCD) has a unique feature - it possess the property of asymptotic freedom which implies that at very high temperatures and/or densities nuclear matter will convert to a deconfined state of quarks and gluons [1]. Recent lattice QCD based calculations [2] indicate that the value of the temperature for the nuclear matter to QGP transition $\sim$ 175 MeV. It is expected that such high temperature can be achieved in the laboratory by colliding nuclei at RHIC and LHC energies.

A high multiplicity system of deconfined quarks and gluons with power law type of momentum distributions can created just after the nuclear collisions at high energies. Interactions among these constituents may alter the momentum distribution of quarks and gluons from a power law to an exponential one - resulting in a thermalized state of quarks and gluons with initial temperature, T_i. This thermalized system with high internal pressure expands very fast as a consequence it cools and reverts to hadronic matter at a temperature, $T_c \sim 175$ MeV. The hadrons formed after the hadronization of quarks may maintain thermal equilibrium among themselves until the expanding system becomes too dilute to support collectivity at a temperature, $T_F(\sim 120$ MeV) called freeze-out temperature from where the hadrons fly freely from the interaction zone to the detector.

The electromagnetic (EM) probes [3] (see [4–6] for review) *i.e.* real photons and dileptons can be used to follow the evolution of the system from the pristine partonic stage to the final hadronic stage through an intermediary phase transition or cross over. In the state of QGP some of the symmetries of the physical vacuum may either be restored or broken - albeit transiently. The electromagnetic probes, especially the lepton pairs can be used very effectively to investigate whether these symmetries in the system are restored/broken at any stage of the evolving matter. Results from theoretical calculations will be shown in the presentation to demonstrate this aspect of the electromagnetically interacting probes. We will demonstrate that lepton pairs can be used very effectively to probe the collective motion (radial and elliptic) of the system.

The other promising probe of the QGP that will be discussed here - is the depletion of the transverse momentum spectra of energetic quarks (and gluons) in QGP. The magnitude of the depletion can be used to estimate the transport coefficients of QGP which is turn can be used to understand the fluidity of the matter.

The transport coefficients of QGP and hot hadrons calculated by using perturbative QCD and effective field theory respectively have been applied to evaluate the nuclear suppression ($R_{\rm AA}$) of heavy flavours. Theoretical results on $R_{\rm AA}$ will be compared with the experimental data available from RHIC and LHC energies. The azimuthal asymmetry of

the system estimated through the single leptons originating from the decays of open heavy flavours produced from the fragmentation of heavy quarks will also be discussed.

2. The electromagnetic probes

The dilepton production per unit four-volume from a thermal medium produced in heavy ion collisions is well known to be given by:

$$\frac{dN}{d^4pd^4x} = -\frac{\alpha^2}{6\pi^3p^2}L\left(M^2\right)f_{BE}(p_0)g^{\mu\nu} \times W_{\mu\nu}\left(p_0,\vec{p}\right) \quad (1)$$

where the factor $L(M^2) = (1+2m_l^2/M^2)\,(1-4m_l^2/M^2)^{1/2}$ is of the order of unity for electrons, $M(=\sqrt{p^2})$ being the invariant mass of the pair and the hadronic tensor $W_{\mu\nu}$ is defined by

$$W_{\mu\nu}(p_0,\vec{p}) = \int d^4x\, e^{ip\cdot x}\langle[J_\mu^{em}(x), J_\nu^{em}(0)]\rangle \quad (2)$$

where $J_\mu^{em}(x)$ is the electromagnetic current and $\langle . \rangle$ indicates ensemble average. For a deconfined thermal medium such as the QGP, Eq. (1) leads to the standard rate for lepton pair productions from $q\bar{q}$ annihilation at lowest order.

The production of low mass dileptons from the decays of light vector mesons in the hadronic matter can be obtained as (see [7] for details):

$$\frac{dN}{d^4pd^4x} = -\frac{\alpha^2}{6\pi^3p^2}f_{BE}(p_0)g^{\mu\nu} \times \sum_{R=\rho,\omega,\phi} K_R\rho_{\mu\nu}^R(p_0,\vec{p}) \quad (3)$$

where f_{BE} is the thermal distributions for bosons, $\rho_{\mu\nu}^R(q_0,\vec{q})$ is the spectral function of the vector meson $R(=\rho,\omega,\phi)$ in the medium, $K_R = F_R^2m_R^2$, m_R is the mass of R and F_R is related to the decay of R to lepton pairs.

The interaction of the vector mesons with the hadrons in the thermal bath will shift the location of both the pole and the branch cuts of the spectral function - resulting in mass modification or broadening - which can be detected through the dilepton measurements and may be connected with the restoration of chiral symmetry in the thermal bath. In the present work the interaction of ρ with thermal π,ω, a_1, h_1 [7, 8] and nucleons [9] have been considered to evaluate the in-medium spectral function of ρ. The finite temperature width of the ω spectral function has been taken from [10].

To evaluate the dilepton yield from a dynamically evolving system produced in heavy ion collisions (HIC) one needs to integrate the fixed temperature production rate given by Eq. 3 over the space time evolution of the system - from the initial QGP phase to the final hadronic freeze-out state through a phase transition in the intermediate stage. We assume that the matter is formed in QGP phase with zero net baryon density at temperature T_i in HIC. Ideal relativistic hydrodynamics with boost invariance [11] has been applied to study the evolution of the system.

The EoS required to close the hydrodynamic equations is constructed by taking results from lattice QCD for high T [2] and hadron resonance gas comprising of all the hadronic resonances up to mass of 2.5 GeV [12, 13] for lower T. The system is assumed to get out of chemical equilibrium at $T = T_{ch} =$ 170 MeV [14]. The kinetic freeze-out temperature $T_F = 120$ MeV fixed from the p_T spectra of the produced hadrons.

A. Invariant mass spectra of lepton pairs

The M distribution of lepton pairs originating from QM and HM (with and without medium effects on the spectral functions of ρ and ω) are displayed in Fig. 1. We observe that for $M > M_\phi$ the QM contributions dominate. For $M_\rho \lesssim M \lesssim M_\phi$ the HM shines brighter than QM. For $M < M_\rho$, the HM (solid line) over shines the QM due to the enhanced contributions primarily from the medium induced broadening of ρ spectral function. However, the contributions from QM and HM become comparable in this M region if the medium effects on ρ spectral function is ignored (dotted line). Therefore, the results depicted in Fig. 1 indicate that a suit-

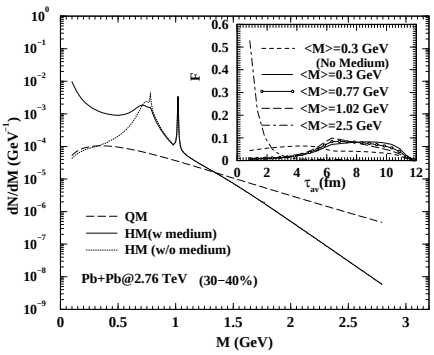

FIG. 1: Invariant mass distribution of dileptons from hadronic matter (HM) for modified and unmodified ρ meson.

able choice of M window will enable us to unravel the contributions from a particular phase (QM or HM). An appropriate choice of M window will also allow us to extract the medium induced effects.

To further quantify these points we evaluate the following [15]:

$$F = \frac{\int' \left(\frac{dN}{d^4x d^2p_T dM^2 dy}\right) dx dy d\eta \tau d\tau d^2p_T dM^2}{\int \left(\frac{dN}{d^4x d^2p_T dM^2 dy}\right) dx dy d\eta \tau d\tau d^2p_T dM^2}$$

where the M integration in both the numerator and denominator are performed for selective windows from M_1 to M_2 with mean M defined as $\langle M\rangle = (M_1+M_2)/2$. While in the denominator the integration is done over the entire lifetime, the prime in $\int'$ in the numerator indicates that the τ integration in the numerator is done from $\tau_1 = \tau_i$ to $\tau_2 = \tau_i + \Delta\tau$ with incremental $\Delta\tau$ until τ_2 attains the life time of the system. In the inset of Fig. 1 F is plotted against $\tau_{\rm av}(= (\tau_1 + \tau_2)/2)$. The results substantiate that pairs with high $\langle M\rangle \sim 2.5$ GeV originate from early time ($\tau_{av} \lesssim 3$ fm/c, QGP phase) and pairs with $\langle M\rangle \sim 0.77$ GeV mostly emanate from late hadronic phase ($\tau_{av} \geq 4$ fm/c). The change in the properties of ρ due to its interaction with thermal hadrons in the bath is also visible through F evaluated for $\langle M\rangle \sim 0.3$ GeV with and without medium effects.

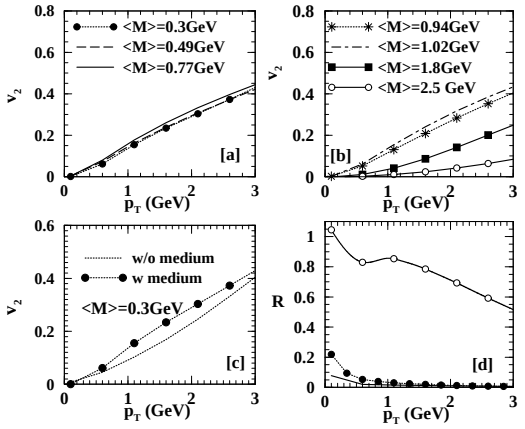

FIG. 2: [a] and [b] indicate elliptic flow of lepton pairs as a function of p_T for various M windows. [c] displays the effect of the broadening of ρ spectral function on the elliptic flow for $\langle M\rangle = 300$ MeV. [d] shows the variation of R (see text) with p_T for $\langle M\rangle = 0.3$ GeV, 0.77 GeV and 2.5 GeV.

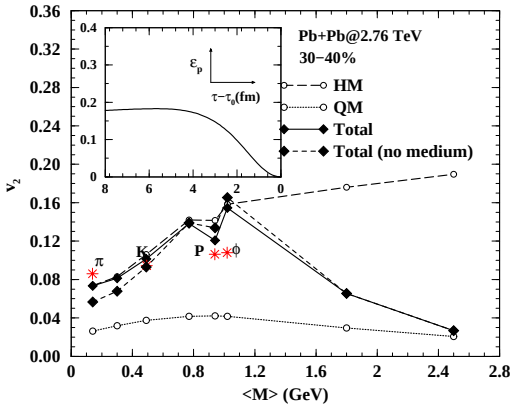

FIG. 3: Variation of dilepton elliptic flow as function of $\langle M\rangle$ for QM, HM (with and without medium effects) and for the entire evolution. The inset shows the variation of momentum space anisotropy with proper time.

B. Elliptic flow of lepton pairs

The elliptic flow of dilepton, $v_2(p_T, M)$ can be defined as:

$$v_2 = \frac{\sum \int cos(2\phi) \left(\frac{dN}{d^2p_T dM^2 dy}|_{y=0}\right) d\phi}{\sum \int \left(\frac{dN}{d^2p_T dM^2 dy}|_{y=0}\right) d\phi} \quad (4)$$

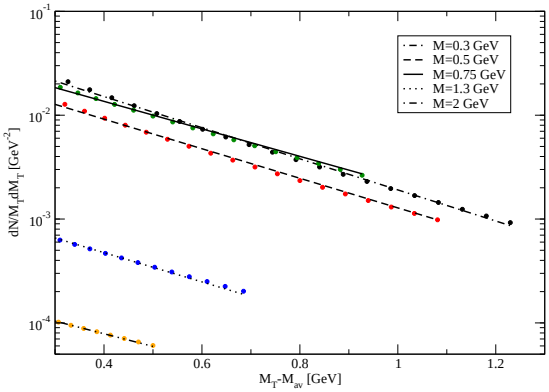

FIG. 4: The dilepton yield plotted against $M_T - M_{av}$ for different M windows for LHC initial condition.

where the $\sum$ stands for summation over QM and HM phases.

Fig. 2 ([a] and [b]) show the differential elliptic flow, $v_2(p_T)$ of dileptons arising from various $\langle M\rangle$ domains. We observe that for $\langle M\rangle = 2.5$ GeV v_2 is small for the entire p_T range because these pairs arise from the early epoch (see inset of Fig. 1) when the flow is not developed entirely. However, the v_2 is large for $\langle M\rangle = 0.77$ GeV as these pairs originate predominantly from the late hadronic phase when the flow is fully developed. It is also interesting to note that the medium induced enhancement of ρ spectral function provides a visible modification in v_2 for dileptons below ρ peak (Fig. 2 [c]). The medium-induced effects lead to an enhancement of v_2 of lepton pairs which is culminating from the 'extra' interaction (absent when a vacuum ρ is considered) of the ρ with other thermal hadrons in the bath. In Fig. 2 [d] we depict the variation of R with p_T for $\langle M\rangle = 0.3$ GeV (solid circle) 0.77 GeV (solid line) and 2.5 GeV (open circle), the quantity R is defined as $R = v_2^{QM} \times f_{QM}/v_2$, where $v_2^{\rm i}$ is the elliptic flow and $f_{\rm i}$ is the fractional yield of dileptons of the phase i. The results clearly illustrate that v_2 of lepton pairs in the large $\langle M\rangle$ domain originate from QM.

Fig. 3 shows p_T integrated elliptic flow, $v_2(\langle M\rangle)$ evaluated for different $\langle M\rangle$ windows defined above. The v_2 (which is proportional to momentum space anisotropy, ϵ_p) of QM is small because the pressure gradient is not fully developed in the QGP phase as evident from the inset plot of ϵ_p with τ. The hadronic phase v_2 has a peak around ρ pole indicating large flow at late times. For $\langle M\rangle > m_\phi$ the v_2 obtained from the combined phases approach the value corresponding to the v_2 for QGP. Therefore, measurement of v_2 for large $\langle M\rangle$ will bring information of the properties of the QGP. It is important to note that the p_T integrated $v_2(\langle M\rangle)$ of lepton pairs with $\langle M\rangle \sim m_\pi, m_K$ is close to the hadronic v_2^π and v_2^K if the thermal effects on ρ properties are included. Exclusion of medium effects give lower v_2 for lepton pairs compared to hadrons. We also observe that the variation of $v_2(\langle M\rangle)$ with $\langle M\rangle$ has a structure similar to dN/dM vs M. As indicated by Eq. 1 we can write $v_2(\langle M\rangle) \sim \sum v_2^{\rm i} \times f_{\rm i}$. The structure of dN/dM is reflected in $v_2(\langle M\rangle)$ through f_i.

C. Radial flow of dileptons

The transverse mass distributions of the lepton pairs at LHC is displayed in Fig. 4. The variation of inverse slope (deduced from the from the transverse mass distributions of lepton pairs, Fig. 4) with $\langle M\rangle$ for LHC is depicted in Fig. 5. The radial flow in the system is responsible for the rise and fall of T_{eff} with $\langle M\rangle$ (solid line) in the mass region ($0.5 <$ M(GeV)$<$ 1.3), for $v_T = 0$ (dashed line) a completely different behaviour is obtained.

D. Radial flow from HBT interferometry of lepton pairs

It was shown in Ref. [16] that the variation of HBT radii (R_{side} and R_{out}) extracted from the correlation of dilepton pairs with $\langle M\rangle$ can used to extract collective properties of the evolving QGP. While the radius (R_{side}) corresponding to q_{side} is closely related to the transverse size of the system and considerably affected by the collectivity, the radius (R_{out}) corresponding to q_{out} measures both the transverse size and duration of particle emission. The extracted R_{side} and R_{out} for different $\langle M\rangle$ are shown in Fig. 6. The R_{side} shows non-monotonic dependence on M, starting from a value close to QGP value

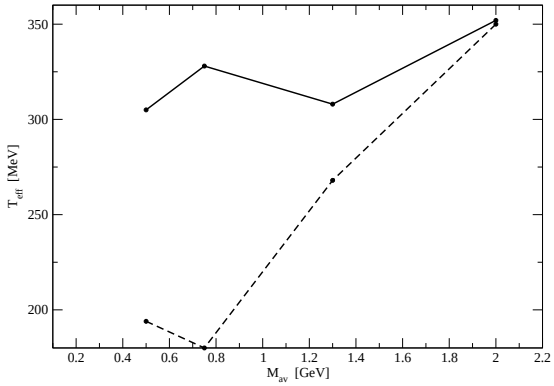

FIG. 5: T_{eff} for different values of the M-bins for LHC conditions. The dashed line is obtained by setting $v_T = 0$.

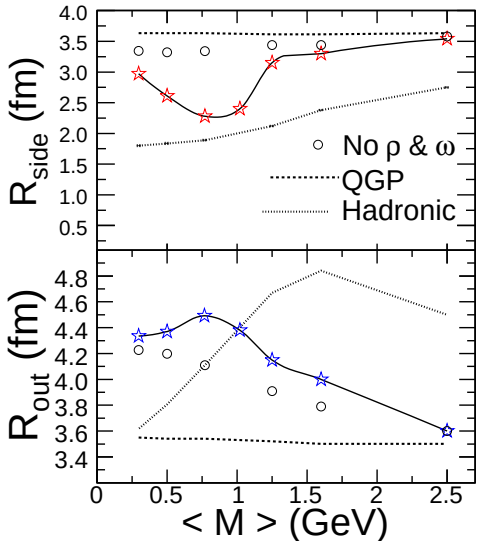

FIG. 6: R_{side} and R_{out} as a function of $\langle M \rangle$. The dashed, dotted and the solid line (with asterisk) indicate the HBT radii for the QGP, hadronic and total dilepton contributions from all the phases respectively. The solid circles are obtained by switching off the contributions from ρ and ω.

(indicated by the dashed line) it drops with increase in M finally again approaching the QGP value for $\langle M \rangle > m_\phi$. It can be shown that $R_{side} \sim 1/(1 + E_{collective}/E_{thermal})$. In the absence of radial flow, R_{side} is independent of q_{side}. With the radial expansion of the system a rarefaction wave moves toward the center of the cylindrical geometry as a consequence the radial size of the emission zone decreases with time. Therefore, the size of the emission zone is larger at early times and smaller at late time. The high $\langle M \rangle$ regions are dominated by the early partonic phase where the collective flow has not been developed fully *i.e.* the ratio of collective to thermal energy is small hence show larger R_{side} for the source. In contrast, the lepton pairs with $M \sim m_\rho$ are emitted from the late hadronic phase where the size of the emission zone is smaller due to larger collective flow giving rise to a smaller R_{side}. The ratio of collective to thermal energy for such cases is quite large, which is reflected as a dip in the variation of R_{side} with $\langle M \rangle$ around the ρ-mass region (Fig. 6 upper panel). Thus the variation of R_{side} with M can be used as an efficient tool to measure the collectivity in various phases of matter. The dip in R_{side} at $\langle M \rangle \sim m_\rho$ is due to the contribution dominantly from the hadronic phase. The dip, in fact vanishes if the contributions from ρ and ω is switched off (circle in Fig. 6).

We observe that by keeping the ρ and ω contributions and setting radial velocity, $v_r = 0$, the dip in R_{side} vanishes, confirming the fact that the dip is caused by the radial flow of the hadronic matter. Therefore, the value of R_{side} at $\langle M \rangle \sim m_\rho$ may be used to estimate the average v_r in the hadronic phase.

The R_{out} probes both the transverse dimension and the duration of emission as a consequence unlike R_{side} it does not remain constant even in the absence of radial flow and its variation with M is complicated. The large M regions are populated by lepton pairs from early partonic phase where the effect of flow is small and the duration of emission is also small - resulting in smaller values of R_{out}. For lepton pair from $M \sim m_\rho$ the flow is large which could have resulted in a dip as in R_{side} in this M region. However, R_{out} probes the duration of emission too which is large for hadronic phase. The larger duration compensates the

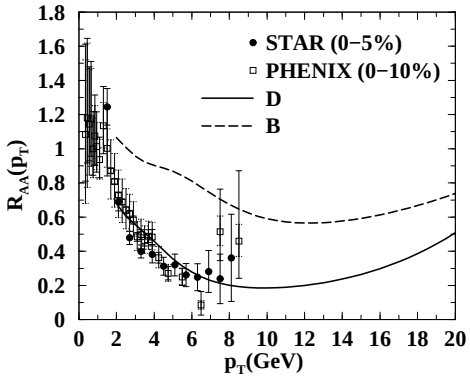

FIG. 7: R_{AA} as a function of p_T for D and B mesons at LHC. Experimental data taken from [23].

reduction of R_{out} due to flow in the hadronic phase resulting in a bump in R_{out} for $M \sim m_\rho$ (Fig. 6 lower panel). Both R_{side} and R_{out} approach QGP values for $\langle M \rangle \sim 2.5$ GeV implying dominant contributions from partonic phase.

3. Suppression of heavy flavours in QGP

The depletion of hadrons with high transverse momentum (p_T) produced in Nucleus + Nucleus collisions with respect to those produced in proton + proton (pp) collisions has been considered as a signature of QGP formation. The two main processes which cause the depletion are (i) the elastic collisions and (ii) the radiative loss or the inelastic collisions of the high energy partons with the quarks, anti-quarks and gluons in the thermal bath.

In the present work we focus on the energy loss of heavy quarks in QGP in deducing the properties of the medium. Because (i) the abundance of charm and bottom quarks in the partonic plasma for the expected range of temperature to be attained in the experiments is small, consequently the bulk properties of the plasma is not decided by them and (ii) they produce early and therefore, can witness the entire evolution history. Hence heavy quarks may act as an efficient probe for the diagnosis of QGP. The depletion of heavy quarks in QGP has gained importance recently in view of the measured nuclear suppression in the p_T spectra of non-photonic single electrons [17, 18].

We assume here that the light quarks and gluons thermalize before heavy quarks. The charm and bottom quarks execute Brownian motion [19] (see references therein) in the heat bath of QGP. Therefore, the interaction of the heavy quarks with QGP may be treated as the interactions between equilibrium and non-equilibrium degrees of freedom. The Fokker-Planck (FP) equation provide an appropriate framework for the evolution of the heavy quark in the expanding QGP heat bath which can be written as [19]:

$$\begin{aligned}\frac{\partial f}{\partial t} &= C_1(p_x,p_y,t)\frac{\partial^2 f}{\partial p_x^2} + C_2(p_x,p_y,t)\frac{\partial^2 f}{\partial p_y^2} \\ &+ C_3(p_x,p_y,t)\frac{\partial f}{\partial p_x} + C_4(p_x,p_y,t)\frac{\partial f}{\partial p_y} \\ &+ C_5(p_x,p_y,t) f + C_6(p_x,p_y,t). \quad . \quad (5)\end{aligned}$$

where,

$$C_1 = D \quad (6)$$

$$C_2 = D \quad (7)$$

$$C_3 = \gamma\, p_x + 2\,\frac{\partial D}{\partial p_T}\,\frac{p_x}{p_T} \quad (8)$$

$$C_4 = \gamma\, p_y + 2\,\frac{\partial D}{\partial p_T}\,\frac{p_y}{p_T} \quad (9)$$

$$C_5 = 2\,\gamma + \frac{\partial \gamma}{\partial p_T}\,\frac{p_x^2}{p_T} + \frac{\partial \gamma}{\partial p_T}\,\frac{p_y^2}{p_T} \quad (10)$$

$$C_6 = 0 \ . \quad (11)$$

where the momentum, $\mathbf{p} = (\mathbf{p}_T, p_z) = (p_x, p_y, p_z)$, γ is the drag coefficient and D is the diffusion coefficient. We numerically solve Eq. 5 [20] with the boundary conditions: $f(p_x,p_y,t) \to 0$ for p_x,$p_y \to \infty$ and the initial (at time $t = \tau_i$) momentum distribution of charm and bottom quarks are taken MNR code [21].

The system under study has two components. The equilibrium component, the QGP comprising of the light quarks and the gluons. The non-equilibrium component, the heavy quarks produced due to the collision

of partons of the colliding nuclei has momentum distribution determined by the perturbative QCD (pQCD), which evolves due to their interaction with the expanding QGP background. The evolution of the heavy quark momentum distribution is governed by the FP equation. The interaction of the heavy quarks with the QGP is contained in the drag and diffusion coefficients. The drag and diffusion coefficients are provided as inputs, which are, in general, dependent on both temperature and momentum. The evolution of the temperature of the background QGP with time is governed by relativistic hydrodynamics. The solution of the FP equation at the (phase) transition point for the charm and bottom quarks gives the (quenched) momentum distribution of hadrons (B and D mesons) through fragmentation. The fragmentation of the initial momentum distribution of the heavy quarks results in the unquenched momentum distribution of the B and D mesons. The ratio of the quenched to the unquenched p_T distribution is the nuclear suppression factor which is experimentally measured. The quenching is due to the dragging of the heavy quark by QGP. Hence the properties of the QGP can be extracted from the suppression factor.

A. Nuclear suppression factor

The variation of the nuclear suppression factor, R_{AA} [19] with p_T of the electron originating from the decays of D and B mesons have been displayed in Fig. 7 for RHIC initial condition ($T_i = 300$ MeV). A less suppression of B is observed compared to D. The theoretical results show a slight upward trend for p_T above 10 GeV both for mesons containing charm and bottom quarks. Similar trend has recently been experimentally observed for light mesons at LHC energy [22]. This may originate from the fact that the drag (and hence the quenching) for charm and bottom quarks are less at higher momentum.

The same formalism is extended to evaluate the nuclear suppression factor, R_{AA} both for charm and bottom at LHC energy. Result has been compared with the recent ALICE data(Ref. [23]) in Fig. 8. The data is reproduced well by assuming formation of QGP

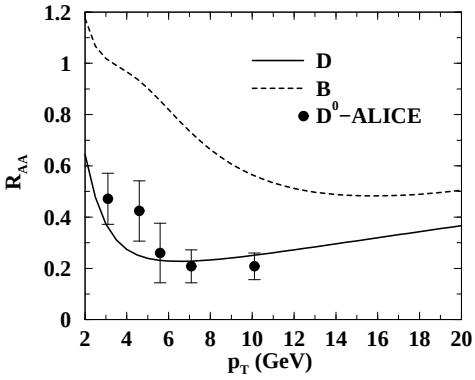

FIG. 8: R_{AA} as a function of p_T for D and B mesons at LHC. Experimental data taken from [23].

at an initial temperature $\sim$ 550 MeV after Pb+Pb collisions at $\sqrt{s_{\rm NN}} = 2.76$ TeV.

B. Elliptic flow of heavy flavours

In Fig. 9 we compare the experimental data obtained by the PHENIX [24] collaborations for Au + Au minimum bias collisions at $\sqrt{s_{NN}} = 200$ GeV with theoretical results obtain in the present work. We observe that the data can be reproduced by including both radiative and collisional loss with $c_s = 1/\sqrt{4}$. In this case v_2^{HF} first increases and reaches a maximum of about 7% then saturates for $p_T > 2$ GeV. However, with ideal equation of state ($c_s^2 = 1/3$) we fail to reproduce data. This is because with larger value of c_s the system expands faster as a result has shorter life time for fixed T_i and T_c. Consequently the heavy quarks get lesser time to interact with the expanding thermal system and fails to generate enough flow. From the energy dissipation we have evaluated the shear viscosity (η) to entropy (s) density ratio using the relation [25]: $\eta/s \sim 1.25T^3/\hat{q}$, where $\hat{q} = \langle p_T^2\rangle/L$ and $dE/dx \sim \alpha_s\langle p_T^2\rangle$ [26], L is the length traversed by the heavy quark. The average value of $\eta/s \sim 0.1-0.2$, close to the AdS/CFT bound [27].

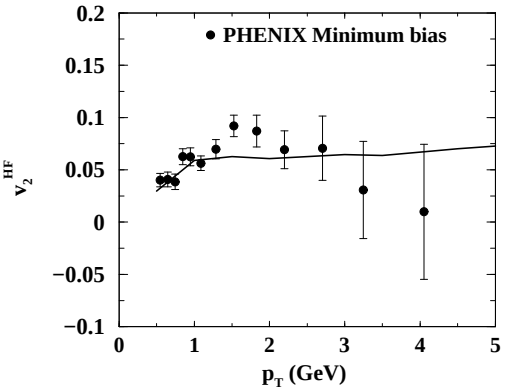

FIG. 9: Elliptic flow of single electrons originating from the heavy mesons decays.

4. Summary

In this work we have discussed the productions of lepton pairs from nuclear collisions at relativistic energies and shown that lepton pairs can trace the evolution of collectivity of the system. The elliptic flow and the nuclear suppression factor of the electrons originating from the heavy flavour decays have been studied by including both the radiative and the collisional processes of energy loss in evaluating the effective drag and diffusion coefficients of the heavy quarks. The results have been compared with the available experimental data and properties of QGP formed at RHIC collisions have been extracted.

Acknowledgment: The author is grateful to Trambak Bhattacharyya, Santosh K Das, Sabyasachi Ghosh, Surasree Mazumder, Bedangadas Mohanty, Payal Mohanty and Sourav Sarkar for collaboration and to Tetsufumi Hirano for providing hadronic chemical potentials.

References

[1] J. C. Collins and M.J. Perry, Phys. Rev. Lett. **34**, 1353 (1975).
[2] S. Borsanyi *et al.* JHEP **1011**, 077 (2010).
[3] L. D. McLerran and T. Toimela, Phys. Rev. D **31** (1985) 545
[4] R. Rapp and J. Wambach, Adv. Nucl. Phys. **25** (2000) 1.
[5] J. Alam, S. Raha and B. Sinha, Phys. Rep. **273** (1996) 243.
[6] J. Alam, S. Sarkar, P. Roy, T. Hatsuda and B. Sinha, Ann. Phys. **286** (2001) 159.
[7] S.Ghosh, S. Sarkar and J. Alam, Eur. Phys. J. C **71**, 176 (2011).
[8] S. Ghosh, S. Mallik and S. Sarkar, Eur. Phys. J. C **70** (2010) 251.
[9] V. L. Eletsky, M. Belkacem, P. J. Ellis and J. I. Kapusta, Phys. Rev. C **64**, 035202 (2001).
[10] R. A. Schneider and W. Weise, Phys. Lett. B **515**, 89 (2001).
[11] J. D. Bjorken, Phys. Rev. D **27** , 140(1983).
[12] V. Roy, A. K. Choudhuri, Phys. Lett. B, **703**, 313 (2011).
[13] B. Mohanty and J. Alam, Phys. Rev. C **68**, 064903 (2003).
[14] T. Hirano and K. Tsuda, Phys. Rev. C **66**, 054905 (2002).
[15] P. Mohanty *et al.*, arXiv:1111.2159 [nucl-th].
[16] P. Mohanty, J. Alam and B. Mohanty, Phys.Rev. C **84**, 024903 (2011).
[17] B. I. Abeleb *et al.* (STAR Collaboration), Phys. Rev. Lett. **98**, 192301 (2007).
[18] A. Adare *et al.* (PHENIX Collaboration), Phys. Rev. Lett. **98**, 172301 (2007).
[19] S. Mazumder, T. Bhattacharyya, J. Alam and S. K. Das, Phys.Rev. C **84**, 044901 (2011).
[20] H. M. Antia, Numerical Methods for Scientists and Engineers, Tata McGraw-Hill, 1991.
[21] M. L. Mangano, P. Nason and G. Ridolfi, Nucl. Phys. B **373**, 295 (1992).
[22] Y. J. Lee (for CMS collaboration), Quark Matter, 2011, May 23-28, Annecy, France.
[23] A. Rossi (for ALICE collaboration), J. Phys. G, **38**, 124139 (2011).
[24] S. S. Adler *et al.* (PHENIX Collaboration), Phys. Rev. Lett. **98**, 172301 (2007)
[25] A. Majumder, B. Müller and X. N. Wang, Phys. Rev. Lett. **99**, 192301 (2007).
[26] R. Baier, arXiv hep-ph/0209038.
[27] P. Kovtun, D. T. Son and A. O. Starinets, Phys. Rev. Lett. **94**, 111601 (2005).